



SURFACE LOADING AFFECTS INTERNAL PRESSURE SOURCE CHARACTERISTICS DERIVED FROM VOLCANO DEFORMATION SIGNALS



EGU2010-12520

Ronni Grapenthin^{1*}, F. Sigmundsson², B. Ófeigsson², E. Sturkell³

¹ Geophysical Institute / Alaska Volcano Observatory, Univ. Alaska, Fairbanks, USA

² Nordic Volcanological Institute, University of Iceland, Reykjavík, Iceland

³ Department of Earth Sciences, University of Gothenburg, Göteborg, Sweden

*contact: ronni@gi.alaska.edu

Abstract

We demonstrate the effect of surface loads on the parameters of a hypothetical magma reservoir and outline possibilities to exploit the load signal for the derivation of crustal parameters. We present a first order approach to distinguish between contributions of internal and external deformation sources based on the ratio of radial and vertical deformation. This method is applied to observations made at the Icelandic Hekla volcano for which we estimate an inflating pressure point source at 11.2 km depth prior to the year 2000 eruption. We estimate the crust in the Hekla region to have an elastic plate thickness of 3.5 km and an effective relaxation time of 100 years, i.e. a viscosity of $0.6 - 1.2 \times 10^{18}$ Pa s.

1. Introduction

Deformation of the Earth's surface provides critical information about the migration of material beneath a volcano. The resulting displacements, recorded by geodetic techniques such as GPS or InSAR, are used to infer characteristics of a volcano's plumbing system; critical for hazard mitigation in volcanic regions.

A set of deformation data usually starts the quest for a source model that explains these data best. The impact of surface load dynamics on these data often seems to be neglected, although their impact on the deformation field and characteristics of volcanoes is recognized *e.g.*, Jull and McKenzie (1996), Pinel (2000, 2005), Pagli (2008). We show that a slow gradual viscous response to lava loads emplaced over decades to centuries must also be considered for volcanoes with large lava production. We consider Hekla volcano, Iceland specifically the 1947, 1970, 1980/81, and 1991 eruptions; all of which deposited in a small central area.

2. Surface and internal load models

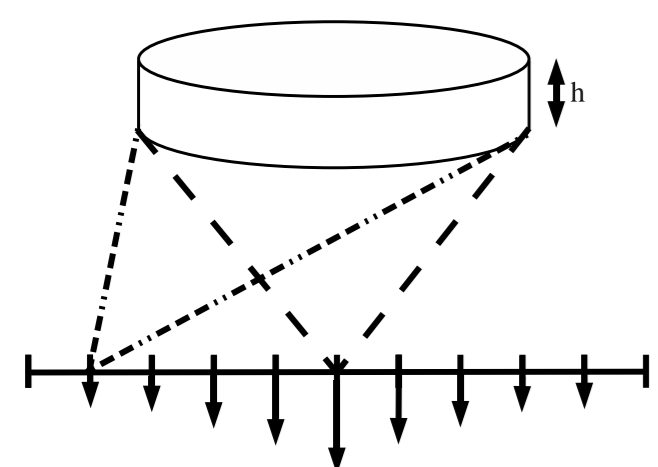


FIG. 1: A Green's function gives unit impulse response to a specific problem. Convolving a Green's function for subsidence with a load will, e.g. result in values for vertical displacement at each grid point.

The emplacement of a **load on the surface** of an Earth in lithostatic equilibrium induces an instantaneous **elastic response**. Given sufficient duration and magnitude or wavelength of the load, a **viscous response** will follow until a final relaxed state is reached. Pinel *et al.* (2007) suggested the use of a single effective relaxation time to model the **transition** from initial to final response for a flat elastic plate overlying a half-space of Newtonian viscosity. They also derived the **Green's functions** (see Fig. 1) which are implemented in the software tool CRUSDE (Grapenthin, 2007) for our **load response modeling**.

An **internal pressure change** in a spherical magma reservoir is described as a **pressure point source** embedded in an **elastic half-space** (Mogi, 1958). This Mogi model depends only on 4 parameters: 3 spatial coordinates of the source's center and its strength (Fig. 2). We also consider deformation due to an oblate rectangular magma body (sill) modeled as a **tensile fault** (Okada, 1992).

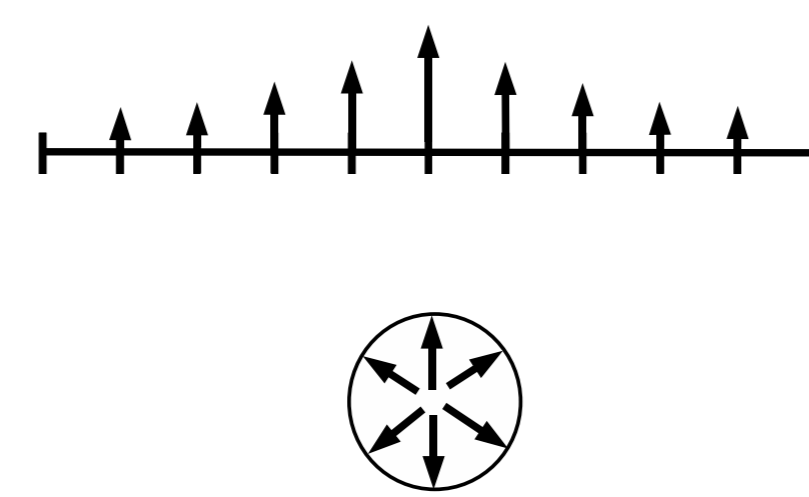


FIG. 2: Vertical displacement field due to pressure point source inflation below the surface.

A combination of **elastic layer and viscous creep** underneath effectively creates a time dependent **low-pass filter** (with Maxwell response time). Hence, short wavelength features of complex loads such as lava flows are lost in recorded deformation pattern. Thus, deformation induced by **surface loads and internal pressure sources** can show **similar**, circular, surface expressions which can be mistaken for one another (see Fig. 3b,c). **Differences**, however, are prominent in the **horizontal field**.

3. Gedankenexperiment & displacement ratios

In Fig. 3b,c we show the effect of a surface load on depth and volume estimates of a magmatic source by superimposing subsidence due to a disk load on deflation of a hypothetical magma reservoir. The inversion of the modulated signal, however, is carried out for the magma reservoir (sill or Mogi source) only and gives considerable misfit.

Fig. 3d shows the ratios $r = \left| \frac{\text{horizontal}}{\text{vertical}} \right|$ displacement for the synthetic data (Pinel, 2007). The ratio of the superimposed data (purple) is clearly distinct from those of the forward and inverse models with a steep slope up to the distance where the horizontal displacement of the Mogi source reaches its maximum.

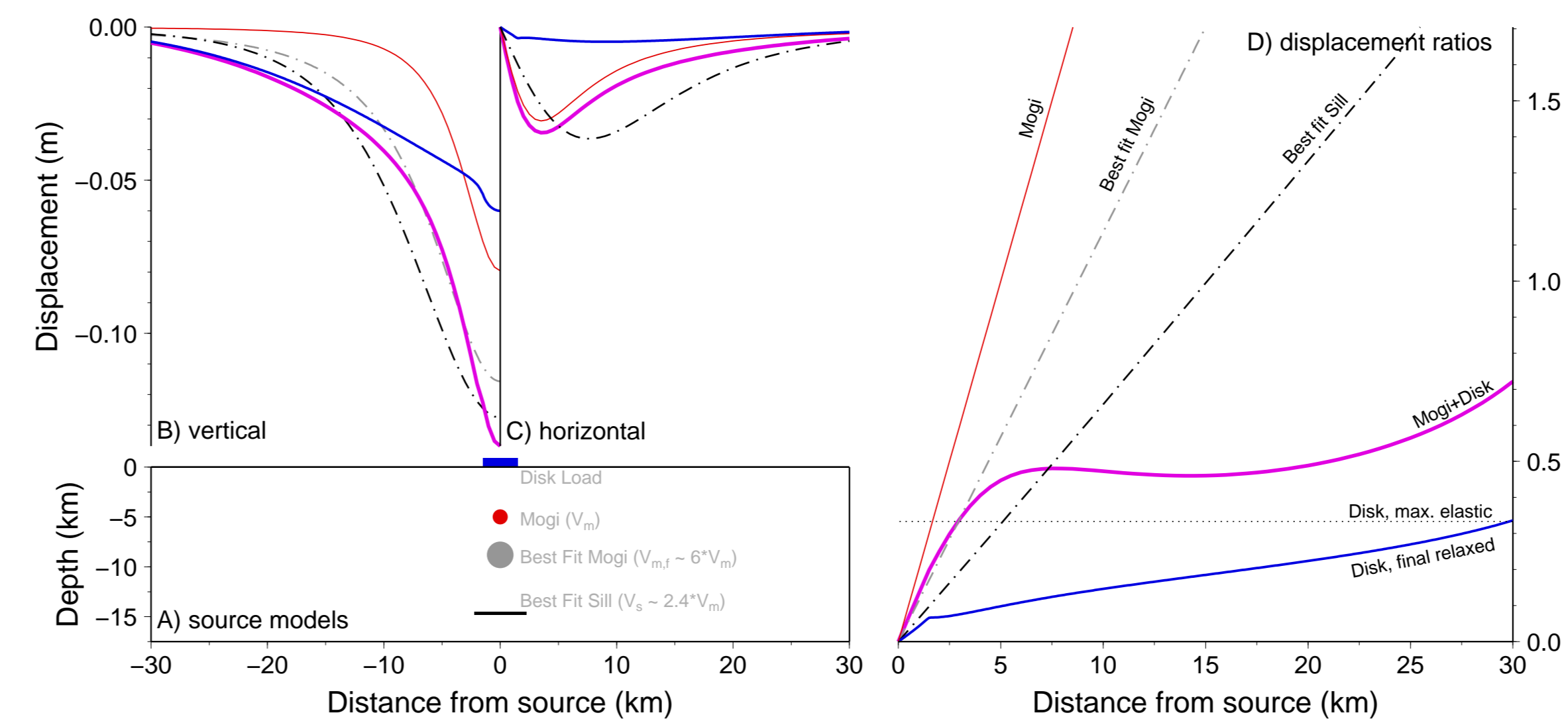


FIG. 3: (A) Forward model sources: Mogi, Disk load. Inversion results: Best fit Mogi, Best fit sill (colors of sources correspond to colors in B,C,D). (B, C) vertical and horizontal deformation due to Disk load emplacement, density $\rho = 2700 \text{ kg m}^{-3}$, radius $r = 1500 \text{ m}$, and uniform height $h = 7.5 \text{ m}$ on a flat surface, deflation of a spherical magma reservoir at depth $d = 5 \text{ km}$ with a volume change $V = -0.025 \text{ km}^3$, superposition of subsidence and deflation. Note similarities in vertical and differences in horizontal field. Inversion of combined signal results in Mogi source at depth $d = 8.8 \text{ km}$ with $V = -0.15 \text{ km}^3$ or a sill at depth $d = 14.8 \text{ km}$, opening $o = 3 \text{ m}$, length and width $l = w = 4.5 \text{ km}$ and volume $V = -0.061 \text{ km}^3$ (D) Displacement ratios $\left| \frac{\text{horizontal}}{\text{vertical}} \right|$ corresponding to sources in A and deformation in B,C. Due to the differences in horizontal displacements at almost similar vertical displacements for surface loading and internal pressure source, this ratio can be used to identify deformation signal superposition.

4. Chamber depth issues – conceptual

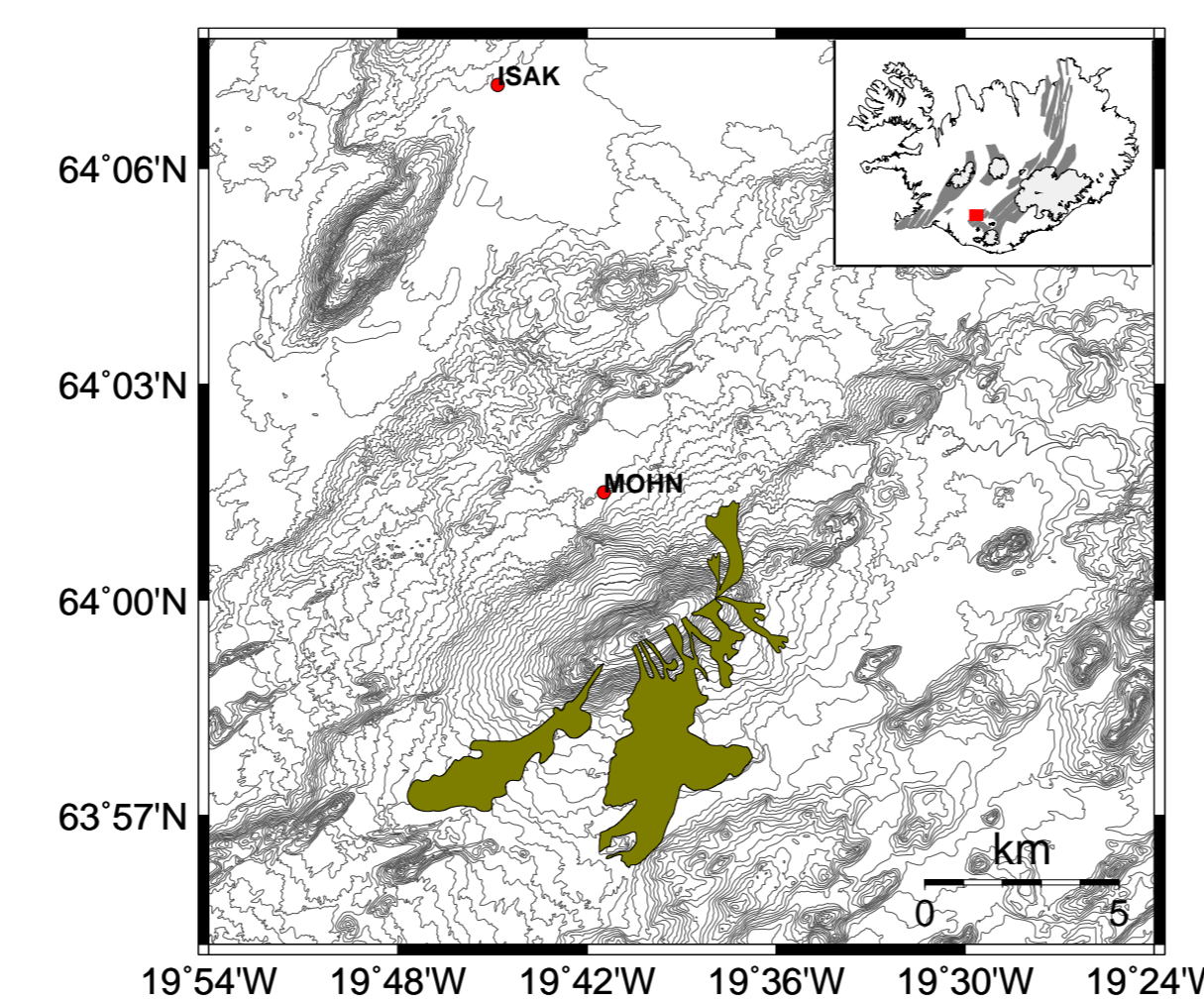


FIG. 4: Map showing Hekla volcano, its location in Iceland (inset), two GPS sites MOHN and ISAK, and preliminary outlines of year 2000 lava.

- consider sites ISAK and MOHN (Fig. 4) after Hekla 2000 eruption ($V=0.189 \text{ km}^3$ lava Höskuldsson *et al.*, 2007).
- note that $r = \left| \frac{U_h}{U_v} \right| = \frac{h}{d}$ for Mogi source (d is source depth, h is horizontal distance from source projected on surface); $h_{\text{mohn}} = 6.2 \text{ km}$, $h_{\text{isak}} = 17 \text{ km}$
- $r_{\text{mohn}} = 0.196$ (camp. data 2000–2004), $r_{\text{isak}} = 0.595$ (cont. data 2002–2006)
- therefore (if post-eruptive deformation was only due to Mogi source): $d = 1/2 * \left(\frac{h_{\text{mohn}}}{r_{\text{mohn}}} + \frac{h_{\text{isak}}}{r_{\text{isak}}} \right) = 30 \text{ km}$
- 30 km is below brittle–ductile transition, previous estimates cluster around $d = 10 \text{ km}$
- indicates: other processes than magma deflation might be involved, suggested mechanism is visco–elastic response to previously erupted lava loads.

5. Derivation of Crustal Parameters for Hekla

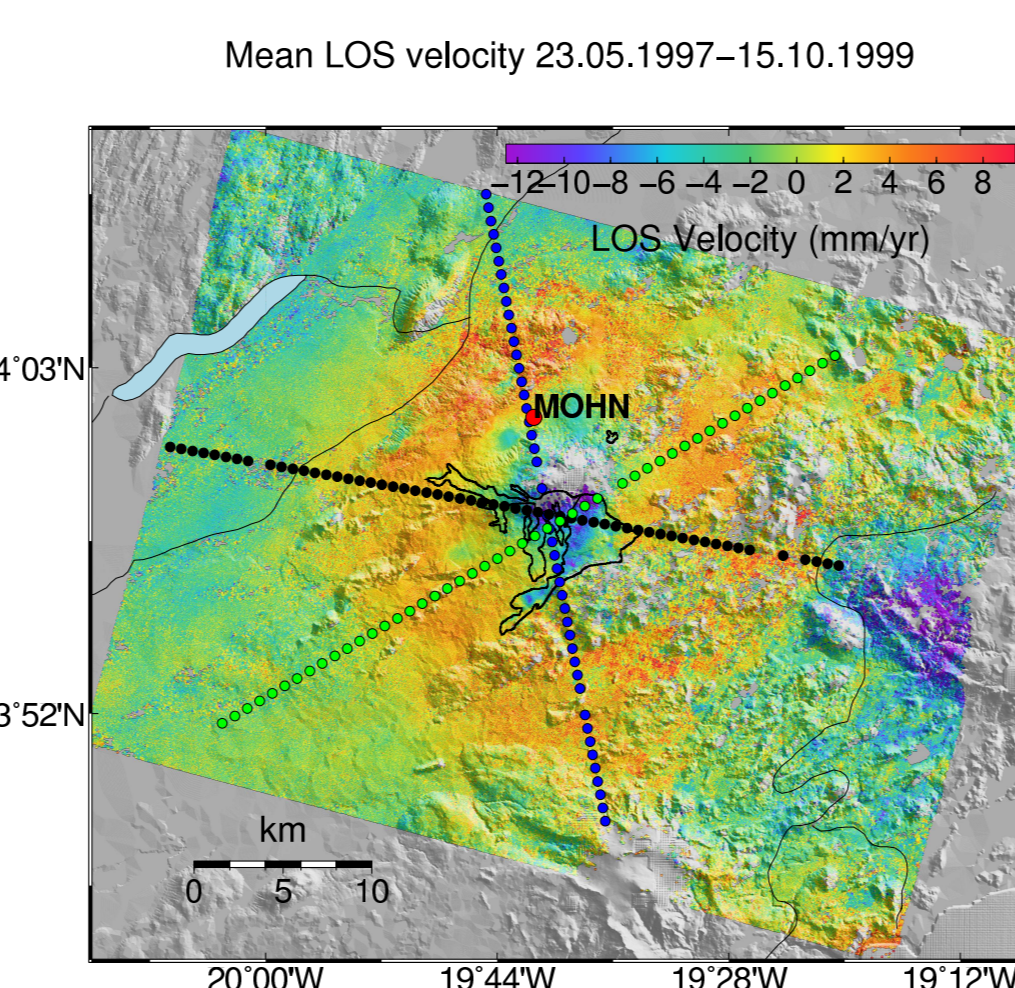


FIG. 5: Mean line of sight (LOS) velocity derived from scenes captured between May 25, 1997 and October 15, 1999. Three obvious deformation areas: circular uplift around Hekla, subsidence in its center (note black 1991 lava flow outline), and subsidence to the ESE of Hekla, likely related to processes at the Torfajökull glacier (ignored). Dots mark points over which the LOS velocity was averaged; profiles shown in Fig. 6.

FIG. 6: Dots show averaged LOS velocity for respective profiles from Fig. 5. Red line is LOS velocity due to a Mogi source fitted to averaged LOS velocities at the "shoulders" of the profiles (depth 11.6 km). Horizontal bars indicate a LOS velocity of 13.5 mm/yr of subsidence surface loading (and other effects?) has to account for.

6. Derivation of Crustal Parameters . . . , Algorithm

- use Young's modulus derived by Grapenthin *et al.* (2006): $E = 40 \text{ GPa}$, Poisson's ratio 0.25
- create profiles of averaged LOS displacement vectors (Fig. 5).
- average a few profile points with significant inflation
- invert for depth ($d=11.2 \text{ km}$) and volume of a Mogi source centered on profile intersection
- estimate difference between expected Mogi max and actual profile min: $m = 13.5 \text{ mm/yr}$; loading has to account for that
- estimate elastic plate thickness H : grid search over the final relaxed responses to 1947–1991 lava loads to fit width of subsidence; get $H = 3.5 \text{ km}$ (agrees with values from previous studies (LaFemina *et al.*, 2005, Pinel *et al.*, 2007) (Fig. 7, left).
- estimate viscosity, η : a grid search over effective relaxation time $t_r = [25 \dots 1000] a$ in $25 a$ increments and fit m ; get $t_r = 100 a$, corresponds to viscosity of $\eta = 0.6 - 1.2 \times 10^{18} \text{ Pa s}$ (agrees with the estimates of $4 - 10 \times 10^{18} \text{ Pa s}$ by Pagli *et al.* (2007) (Fig. 7, right).
- Remove load contribution from InSAR data if so desired.

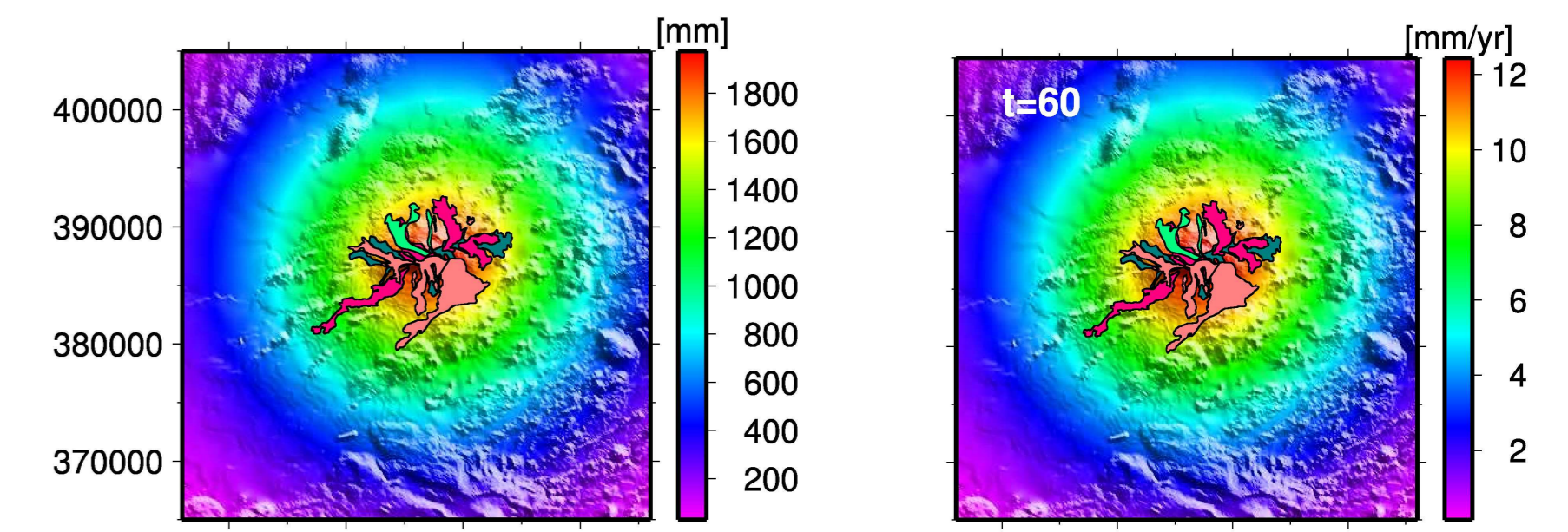


FIG. 7: Vertical displacements after 1947–1991 Hekla flows are applied. Left Final relaxed state. Elastic plate thickness is being varied such that displacement radius fits InSAR observations. Right Displacement rates, effective relaxation is varied until max. displacement rate fits InSAR observations.

7. Conclusions

- surface load signals in volcanic regions affect source model estimates; up to the point of changing the preferred model
- gradual subsidence may be mistaken as source deflation
 - ... or at least has significant impact on interpretations
 - horizontal deformation gives clues about signal source(s)
 - visco-elastic response to (recent) loads must be considered
- signal can be exploited to derive crustal parameters . . .
 - GPS, InSAR, and inverse approaches are necessary
 - we had: Young's modulus, Poisson's ratio
 - we estimated: source depth, elastic plate thickness, viscosity

References: Grapenthin, R., Sigmundsson, F., Geirsson, H., Árnadóttir, T., Pinel, V. (2006) Icelandic rhythmicity: Annual modulation of land elevation and plate spreading by snow load. *Geophys. Res. Lett.*, 33, L24305.
 Grapenthin, R. (2007), CRUSDE: A plug-in based simulation framework for composable CRUSTAL Deformation simulations using Green's functions. *Ms thesis*, Humboldt-Universität zu Berlin, pp. 127.
 Höskuldsson, Á., Óskarsson, N., Pedersen, R., Grönvold, K., Vogfjörð, K., Ólafsdóttir, R. (2007) The millennium eruption of Hekla in February 2000. *Bull. Volc.*, doi:10.1007/s00445-007-0128-3.
 Mogi, K. (1958) Relations between eruptions of various volcanoes and the deformations of the ground surface around them. *Bull. Earthquake Res. Inst. Univ. Tokyo*, 36, 99–134.
 Pinel, V., Sigmundsson F., Sturkell, E., Geirsson, H., Einarsson, P., Gudmundsson, M.T., Högnadóttir, Th. (2007) Discriminating volcano deformation due to magma movements and variable surface loads: Application to Katla subglacial volcano, Iceland. *Geophys. J. Int.*, 169, 325–338.